Performance of Cylinder Head and Piston Head Suction Valve Configurations in Small Variable-Speed Reciprocating Compressors

Willian T F D SILVA[1], Sergio K Lohn[2], Igor L L P Silva[1], Cesar J. DESCHAMPS[1]*

[1]POLO Research Laboratories for Emerging Technologies in Cooling and Thermophysics
Federal University of Santa Catarina
Florianopolis, SC, Brazil

[2]NIDEC Global Appliance, R&D
Joinville, SC, Brazil

* Corresponding Author: deschamps@polo.ufsc.br

ABSTRACT

The suction valve is typically mounted on the cylinder head of small reciprocating compressors. However, with the current trend of compressor miniaturization, positioning the suction valve on the piston head (VOPH) is an alternative to increase the valve passage area. This article presents a study comparing the performance of suction valves placed on the cylinder head versus those on the piston head across different compressor speeds. A validated numerical model was used to simulate the compressor for both configurations under different operating conditions. The results indicate that the dynamics of the suction valve is very sensitive to changes in compressor speed, significantly affecting performance. Furthermore, we found that valves of identical passage area and dynamic properties exhibit inferior performance when mounted on the piston head compared to the cylinder head (VOCH). Despite significantly reducing the compressor's volumetric efficiency, the suction gas superheating associated with the VOPH was not influenced by the compressor speed. The findings of this study provide insights for the design and optimization of variable-speed compressors, focusing efficiency and reliability.

1. INTRODUCTION

Recent trends in compressor technology have focused on miniaturization to meet the increasing demand for compact, efficient, and portable devices. Specifically, the miniaturization of reciprocating compressors involves reducing the size of cylinder heads. This reduction presents challenges, particularly in the design of the suction orifice area, since it regulates the mass flow rate of refrigerant into the compression chamber, a critical factor in compressor efficiency. In fact, as the cylinder head size decreases, the corresponding reduction in the suction orifice size limits the effective flow area available for the suction process, leading to increased head loss and reduced volumetric and isentropic efficiencies.

To address these challenges, recent innovations have included positioning the suction valve directly on the piston head (VOPH), a design change suggested by Wu et al. (2022). They noted that the valve's stiffness on the piston should be greater than that on the cylinder head to prevent excessive lift, and consequently high valve impact velocities. Also, this configuration may lead to increased suction gas superheating losses due to the high temperature of the piston wall, potentially decreasing the volumetric efficiency further.

This article presents a numerical analysis of the performance impacts of locating the suction valve on the piston head. The study uses a model developed by Silva et al. (2022) to simulate a small variable-speed reciprocating compressor adopted in household refrigeration with refrigerant R600a.

2. METHODOLOGY

2.1 Suction Valve on the Piston

The operation of the suction valve in conjunction with the piston head is illustrated Figure 1. As the piston moves past the top dead center, it begins to accelerate downward (I). This acceleration continues through the re-expansion process

until the pressure in the compression chamber equals that in the suction chamber, triggering the opening of the suction valve. The acceleration of the piston brings about inertial forces that facilitate the opening of the valve (II). As the suction process proceeds with the valve open, the piston eventually reaches its maximum velocity. Subsequently, as the piston decelerates, the inertial forces act to push the suction valve towards the piston (III). After the piston reachs the bottom dead center, it starts its upward motion, during which the increasing pressure in the compression chamber acts to close the valve (IV).

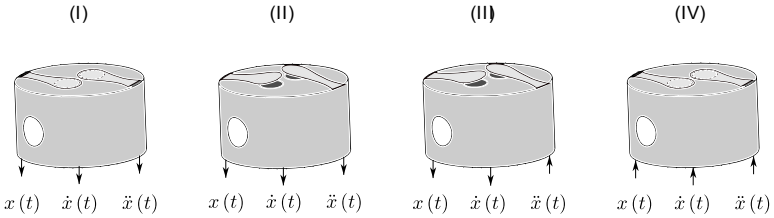

Figure 1: Suction valve on the piston head.

2.1 Simulation model

The compressor simulation model depicted in Fig. 2 was developed using GT-SUITE, a commercial software. This model consists of volumes connected by tubes (SILVA et al., 2022). The piston position at any given time, $x(t)$, is calculated as follows:

$$x(t) = d_{TDC} - \left\{e_c \cos\theta + [L_r^2 - (e_c \sin\theta - d_m)^2]^{1/2}\right\} \quad (1)$$

where d_{TDC}, e_c, L_r and d_m are, respectively, the distance between the top dead center (TDC) and the bottom dead center (BDC), eccentric ratio of the compressor mechanism, length of the connecting rod, and cylinder offset. The volume of the compression chamber at any time can be obtained by multiplying the instantaneous piston position from Eq. (1) by the piston area.

The instantaneous temperature inside the compression chamber is calculated via the first law of thermodynamics, with wall heat transfer estimated based on the correlation proposed by Disconzi et al. (2012). The pressure within the compression chamber is derived from the temperature and specific mass, the latter obtained from mass conservation, and is accessed from the Refprop database (LEMMON, 2018).

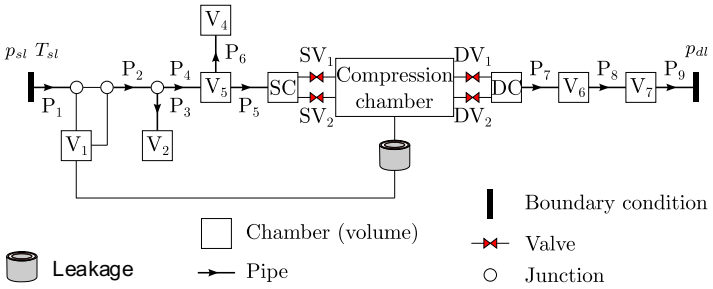

Figure 2: Schematic gas flow structure of the entire simulation compressor model.

Valve dynamics is modeled as a single-degree-of-freedom that includes a spring, damper, and mass. Fluid flow in the suction and discharge mufflers is described by a one-dimensional formulation and solved numerically via the finite volume method (DESCHAMPS et al., 2002), using an explicit time scheme. Mass flow rate through valves is calculated using the concept of effective flow area with reference to one-dimensional isentropic flow in a convergent nozzle, taking into account viscous friction effects (LINK and DESCHAMPS, 2010).

The time-step was constrained by the Courant-Friedrichs-Lewy criterion to be less than 0.7, ensuring the numerical stability of the solution procedure. The boundary conditions adopted in the simulation model included the evaporating and condensing pressures, the temperature at the compressor inlet, and the temperature of the external environment. The solution procedure was considered to have converged when differences in pressure and mass flow rate were less than 0.2% and in temperature less than 0.1 K between two consecutive compression cycles.

2.2 Thermal model

The thermal model used in the simulations is essentially that proposed by Silva et al. (2022), following a hybrid approach in which the compressor is divided into several non-overlapping control volumes. The general equation applied to each control volume has the form of Eq. (1). Details of the compressor components and the non-linear system of equations representing the compressor thermal sub-model are presented in Table 1.

$$\sum \dot{Q} + \sum_{i}^{N} UA_{ij}\left(T_j - T_i\right) = 0, \tag{2}$$

Regarding the valve-on-piston head configuration (VOPH), the thermal model requires some modifications. Although it is assumed that the suction muffler remains unchanged regardless the valve configuration, the treatment of the suction muffler wall temperature must differ. Specifically, when the valve is mounted on the piston, no control volume is adopted for the suction muffler. Consequently, the wall temperature of the suction muffler wall is assumed to match that of the cylinder temperature. Therefore, the control volumes for the compression chamber and the suction muffler are combined into a single control volume, as depicted in Fig. 3.

Table 1:- Energy balances of the compressor thermal network.

Control volume	$\sum \dot{Q}$	$\sum_{i}^{N} UA_{ij}(T_j - T_i)$
Suction muffler	$\dot{Q}_{sm,w}$	$UA_{ie-sm}(T_{ie} - T_{sm,w})$
Compression chamber	$\dot{Q}_{cyl,w} + \dot{Q}_{pc}$	$UA_{ie-wall}(T_{ie} - T_{cyl,w})$
Valve plate	$\dot{Q}_{plate}$	$UA_{dc-plate}(T_{dc} - T_{cyl,plate})$
Discharge chamber	$\dot{Q}_{dc}$	$UA_{dc-plate}(T_{dc} - T_{cyl,plate})$
Discharge muffler	$\dot{Q}_{dm,w}$	$UA_{ie-dm}(T_{ie} - T_{dm,w})$
Discharge tube	$\dot{Q}_{dt,w}$	$UA_{ie-dt}(T_{ie} - T_{dt,w})$
Oil	$\dot{Q}_b$	$UA_{sh-oil}(T_{sh} - T_{oil})$
Motor	$\dot{Q}_m$	$UA_{ie-mot}(T_{ie} - T_m)$
Internal environment	$(1-\varphi)\dot{m}_{sl}(h_{sl} - h_{ie}) + \dot{m}_l(h_l - h_{ie})$	$UA_{ie-sm}(T_{sm,w} - T_{ie}) + UA_{ie-wall}(T_{cil,w} - T_{ie}) + UA_{ie-dm}(T_{dm,w} - T_{ie}) + UA_{dt-ie}(T_{dt,w} - T_{ie}) + UA_{ie-mot}(T_{mot} - T_{ie}) + UA_{ie-sh}(T_{sh} - T_{ie})$
Shell	-	$UA_{sh-oil}(T_{oil} - T_{sh}) + UA_{ie-sh}(T_{ie} - T_{sh}) + UA_{sh-amb}(T_{amb} - T_{sh})$

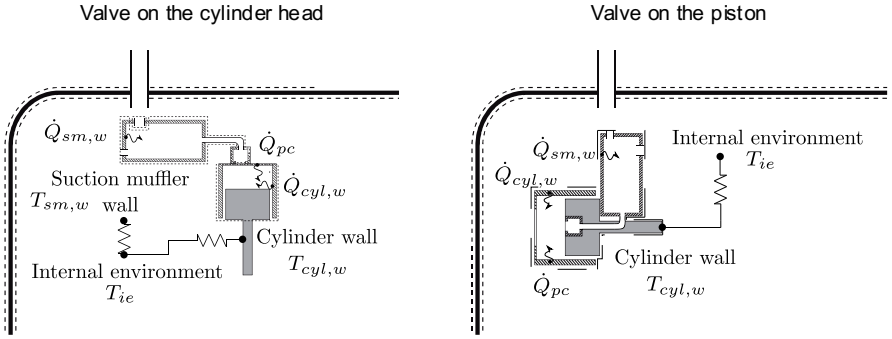

Figure 3: Comparison between thermal model for VOCH (left) and VOPH (right)

2.4 Valve dynamics

Fig. 4 shows a schematic of a single-degree-of-freedom spring-damper-mass system used to simulate a suction valve on a piston subjected to a harmonic motion. Applying D'Alembert's principle, it follows that:

$$M_v\ddot{y} + C_v\dot{y} + K_v y = C_v\dot{x} + K_v x + F_{\Delta p} + F_{st}, \tag{3}$$

where M_v, C_v and K_v are the equivalent mass, damping coefficient and stiffness of the reed valve, respectively. F_{st} is the valve stiction force due to the presence of lubricant oil, as estimated by Pizarro-Recabarren et al. (2013), and $F_{\Delta p}$

is the force resulting from to the pressure load on the reed, calculated using the concept of effective force area (PEREIRA and DESCHAMPS, 2011). Given that the piston position x(t) is known from Eq. (1), the valve dynamics can also be described as:

$$M_v\ddot{y} + C_v\dot{y} + K_v y = F_{pis} + F_{\Delta p} + F_{st}, \tag{4}$$

where:

$$F_{pis} = K_v\left[d_{TDC} - \sqrt{L_r^2 - (e_c\ \sin\theta\ - d_m)^2} - e_c\ \cos\theta\right] + C_v\dot{\theta}\left[\frac{e_c\ \cos\theta\,(e_c\ \sin\theta - d_m)}{\sqrt{c^2 - (e_c\ \sin\theta - d_m)^2}} + e_c\ \sin\theta\right], \tag{5}$$

This relationship indicates that the valve excitation is equivalent to applying a harmonic force F_{pis} to a mass in a fixed reference system. This force is related to the crank angle angular speed, $\dot{\theta}$, which varies with the compressor rotational speed. Hence, the magnitude of the harmonic force and the corresponding inertial effect on the suction valve due to the piston motion are expected to increase with the compressor speed. Naturally, for the configuration of installed in the cylinder head, this type of excitation does not occur and, therefore, F_{pis} = 0.

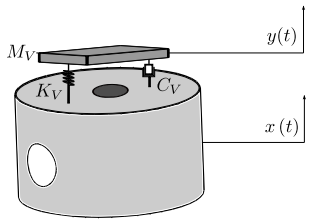

Figure 4: 1d spring-damper-mass system of the valve on the piston.

3. COMPRESSOR THERMODYNAMIC PERFORMANCE

The thermodynamic performance of hermetic reciprocating compressors can be characterized by volumetric efficiency and exergetic efficiency. A procedure has been recently proposed to detach these efficiencies into their main components (physical sub-processes), facilitating identification the primary sources of inefficiencies. As the focus of this paper is the suction valve, the analysis focuses on inefficiencies associated with the suction process.

3.1 Volumetric efficiency

The volumetric efficiency is defined as the ratio of the actual mass flow rate ($\dot{m}$) to the theoretical mass flow rate ($\dot{m}_{th}$). The theoretical mass flow rate assumes an ideal compressor operating without heat transfer or head losses in the suction path, with isobaric intake admission and discharge processes, no backflow, absence of leakage in the compression chamber, no-slip condition in the electric motor, and no clearance volume. The theoretical mass flow rate of can be calculated using the following equation:

$$\dot{m}_{th} = \frac{N\ \rho_{sl}\forall_{sw}}{60}, \tag{6}$$

where N is the nominal rotational speed of the compressor, ρ_{sl} in the gas density at the suction line, and $\forall_{sw}$ is the volume swept by the piston.

Thus, the volumetric efficiency can be expressed as

$$\eta_v = \frac{\dot{m}}{\dot{m}_{th}} = \frac{\dot{m}_{th}\ - \Delta\dot{m}_{total}}{\dot{m}_{th}}, \tag{7}$$

where the actual mass flow rate, $\dot{m}$, can be written as the theoretical mass flow rate minus the total mass flow reduction, $\Delta\dot{m}_{total}$, brought about by various inefficiencies (Santos and Deschamps, 2020; Silva et al., 2022).

3.2 Exergy loss

The second law of thermodynamics allows estimates of energy inefficiencies based on the destruction of exergy, which is equivalent to irreversibility or entropy generation. Exergy represents the maximum useful work that can be obtained as a system approaches equilibrium with a reference environment, known as the dead state. The second law establishes that exergy is preserved in reversible processes and destroyed in actual processes. Like energy, exergy can be transferred between systems through via heat, work, and mass interactions. Therefore, the exergetic efficiency (η_{exe}) of a system is defined as the ratio of the minimum power required (reversible power, $\dot{W}$rev) to the actual power input ($\dot{W}$ele) to change the thermodynamic state of a fluid, that is:

$$\eta_{exe} = \frac{\dot{W}_{rev}}{\dot{W}_{ele}}, \tag{8}$$

The exergetic efficiency can also be expressed as a function of the total exergy loss ($\dot{I}_d$), which can be fractionated into various irreversibilities associated with different processes of a compression cycle. Therefore, the exergetic efficiency of a compressor is calculated by accounting for inefficiencies due to different entropy generation mechanisms:

$$\eta_{exe} = \frac{\dot{W} - \dot{I}_d}{\dot{W}}, \tag{9}$$

Thus, the power supplied to the compressor can be broken down into the reversible power required to perform the different thermodynamic processes and the power lost to irreversibilities that reduce the exergetic efficiency. These irreversibilities can be fractionated among the various components of the compressor. All exergy loss rates (irreversibilities) can be calculated from the entropy generation, $\dot{S}g$, and the dead state temperature, T_0, using the Gouy-Stodola relationship (Eq. 10). For details on the method to estimate all irreversibilities in reciprocating compressors, refer to Araujo and Deschamps (2020).

$$\dot{I} = T_0 \dot{S}_g, \tag{10}$$

4. RESULTS

The main objective of this article is to analyze the performance of compressors employing suction valves located on the cylinder head and on the piston, under identical boundary conditions and across the same range of compressor speeds. The dynamic characteristics of the valves and the area of the suction orifice were the same for both configurations. To assess the differences between both compressor designs, the analysis considered factors such as exergy loss, valve impact velocity, valve displacement, volumetric inefficiencies, and acoustic performance were adopted. The simulations of both designs adopted an ideal discharge valve to avoid any effect of its dynamics on the suction valves. All the results are presenting with a dimensionless rotational speed, defined by the maximum compressor speed, $N^* = N/N_{max}$.

4.1 Valve displacement

Fig. 5 compares the displacements of suction valves mounted on the cylinder (VOCH) and piston (VOPH) heads. The valves open four times during the suction process when the compressor operates at $N^* = 0.3$, and three times at $N^* = 1.0$, regardless the valve's location. Fig. 5a shoes that the displacements of both valves are nearly identical at $N^* = 0.3$, corroborating the findings of Wu et al. (2022). The auxiliary force provided by the piston motion enables the valve to reach maximum lift during the first opening. However, subsequent openings occur as the piston decelerates, which limits the valve's opening. Consequently, the valve on the piston exhibits smaller displacement during the third and fourth openings in comparison with the valve on the cylinder head (VOCH). Despite these differences, both valves close simultaneously.

As illustrated in Fig. 5b, the influence of piston motion is more pronounced at $N^* = 1.0$, and the first opening displacement of the VOPH configuration is slightly greater than that of the VOCH. However, the piston motion significantly reduces subsequent valve displacements, causing the valve on the piston to close earlier than the cylinder head valve, thereby reducing backflow.

The displacement differences between the VOCH and VOPH are quantified using the root-mean-square error (RMSE), as shown in Fig. 6. As the compressor has two different valves, the RMSE for both were calculated and shown by SV1 and SV2. RMSE is a standard metric for assessing the similarity between curves by calculating the average squared differences between the reference values (displacement for VOCH) and observed values (displacement for VOPH). The RMSE is almost negligible at lower speeds but increases with the compressor speed, highlighting that the effects of piston motion on the valve are significant at higher speeds.

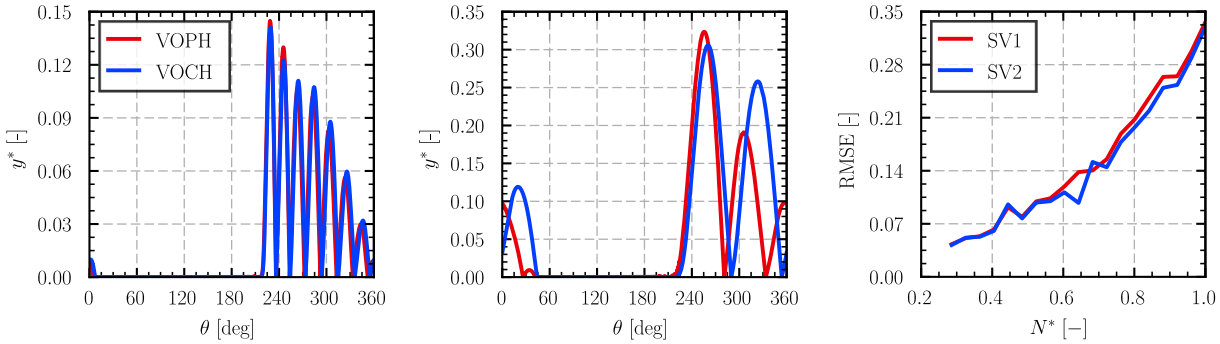

(a) $N^* = 0.3$ (b) $N^* = 1.0$

Figure 6: Displacement of the VOCH and VOPH for two different rotational speeds.

Figure 5: Root mean square error between VOCH and VOPH.

4.2 Valve impact velocity

Valve impact velocity is critical parameter in compressor design, essential for ensuring it does not exceed the reliability limits established for valves. Fig. 7 shows the impact velocity for the SV1 and SV2 tested in both configurations (VOCH and VOPH). The results show that the impact velocity is greater for the valve on the piston (VOPH), particularly at compressor high speeds, due to the larger displacements observed in the first valve oscillation (see Fig. 5).

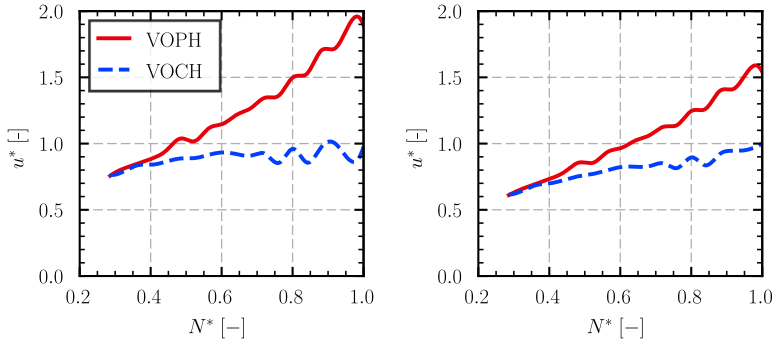

(a) Suction valve 1 (b) Suction valve 2

Figure 7: Comparison between the impact speed for VOCH and VOPH

There is a marked difference in the predicted impact velocities between valve 1 and valve 2 on the cylinder head. In contrast, the difference in impact velocity for the valves on the piston configuration is minimal, indicating that the piston motion has a more significant effect on impact velocity than on valve dynamics. This finding contradicts Wu et al. (2022), who reported a decrease in impact velocity when the valve is mounted on the piston. However, consistent with our analysis, Wu et al. (2022) recommend increasing reed stiffness to minimize valve displacements in the first opening.

4.3 Volumetric efficiency

Fig. 8 shows the volumetric inefficiencies associated with the suction gas path. As depicted in Fig. 8a, the suction valve on the piston (VOPH) exhibits virtually no backflow due to its earlier closure compared to the suction valve on

the cylinder head (VOCH). Nevertheless, Fig. 8b indicates that the volumetric inefficiency of VOPH is higher than that of the VOCH assembly when the compressor operates at speeds exceeding $N^* = 0.6$. This increase of inefficiency can be attributed to the inertial effects of the piston motion, which negatively affect valve dynamics (see Fig. 5b). At lower speeds, the volumetric inefficiency of the VOCH is greater due to the smaller displacement of the first opening, acting to increase the head loss.

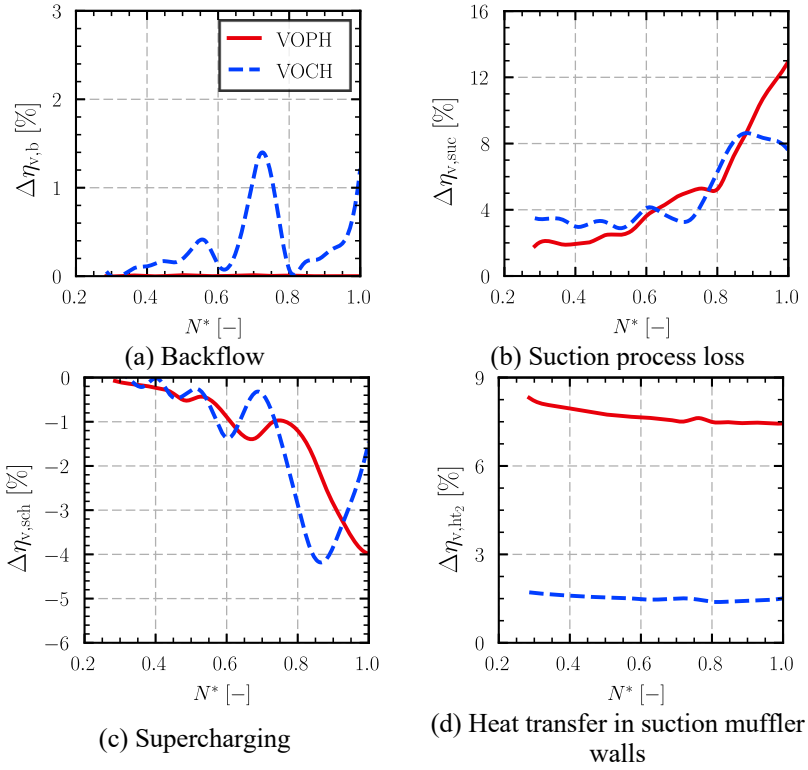

(a) Backflow (b) Suction process loss

(c) Supercharging (d) Heat transfer in suction muffler walls

Figure 8: Volumetric inefficiencies associated with VOCH and VOPH.

Concerning supercharging (Fig. 8c), no significant differences are observed up to approximately $N^* = 0.6$. At higher speeds, a marked difference is clearly seen between the results of both configurations. It is noteworthy that despite the VOPH closing more quickly than the VOCH, the supercharging effect persists since the valve closure occurs after the bottom dead center, particularly at speeds above $N^* = 0.8$, where the supercharging effects for the VOPH are more pronounced.

Fig. 8d shows the inefficiencies due to heat transfer between the gas and the hot walls of the suction muffler. The piston configuration is more prone to inefficiency due to the contact of the gas with the significantly warmer piston walls compared to the walls of the suction muffler. The results also show that this inefficiency remains relatively stable regardless the compressor speed.

The overall volumetric efficiency resulting from the VOPH is consistently lower than that of the VOCH (Fig. 9), due to the higher inefficiencies detailed in Fig. 8. The difference between the two configurations is 3% at minimum speed, but it increases to over 5% at the maximum speed, primarily due to valve fluttering during the suction process (Fig. 8b), which varies with rotational speed.

4.3 Exergy loss

Despite the considerable impact of the suction process on the volumetric efficiency, as illustrated in Fig. 8b, the configuration of the suction valve does not significantly affect the specific exergy loss (i.e., exergy loss per unit mass flow rate), as indicated in Fig. 10a. The VOPH configuration even demonstrates higher exergetic efficiency at rotational speeds below $N^* = 0.5$. This improvement likely stems from reduced mass flow rate due to \volumetric inefficiencies during the suction process, which in turn decreases viscous friction losses. However, above this speed

threshold, the specific exergy loss peaks at 6.28 kJ/kg for the VOPH and 6.04 kJ/kg for the VOCH, a difference of 4%, attributed to the higher mass flow rate in the VOCH.

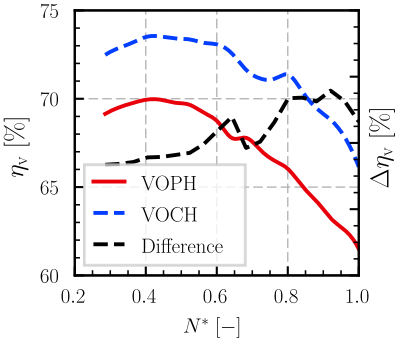

Figure 9 - Overall volumetric efficiency for the compressor with suction valves on the piston and on the cylinder head

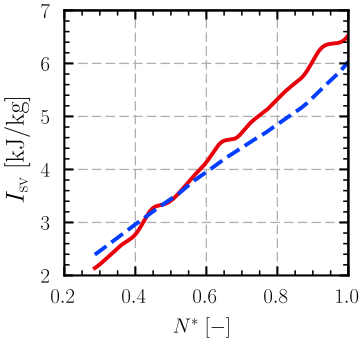

(a) Suction valves

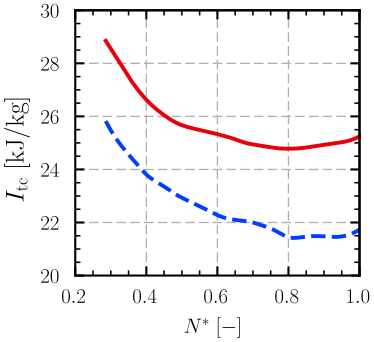

(b) Heat transfer

Figure 10 - Specific exergy losses at the suction valves (a) and due to heat transfer (b) for both valve configurations.

Regarding heat transfer irreversibility, Fig. 10b shows quite different results for the two configurations. Although the inlet temperature of the refrigerant is the same in both configurations, the VOPH generates more entropy during the suction process primarily due to a greater temperature difference between the refrigerant and the walls. This irreversibility decreases with increasing compressor speed, regardless the valve configuration, since higher speeds enhance heat transfer, thereby reducing temperature differences. Notably at the minimum rotational speed, the irreversibility with the VOPH is 17.5% greater than that for the VOCH.

Fig. 11 compares the exergetic efficiencies for both valve configurations. It is important to note that these exergy efficiencies are overestimated due to the assumption of an ideal discharge valve. The exergetic efficiency is consistently higher for the VOCH across the entire range of operating speeds, primarily due to lower heat transfer irreversibility. The efficiency difference remains relatively stable, peaking at 1.9% at $N^* = 0.3$ and dropping to 1.5% at $N^* = 1.0$, with an average difference of 1.7%.

4.4 Acoustic performance

Another crucial aspect of the compressor is its acoustic performance, which is assessed in this study by analyzing pressure pulsations within the suction chamber. Fig. 12 shows minimal differences in pressure pulsation between the two configurations. However, there are noticeable increases in pressure pulsation at specific frequencies (315, 500, 630, 800, and 1250 Hz within the $N^* = 0.9$ scenario). Conversely, the 500 Hz frequency band consistently shows a reduction in pressure pulsations across all rotational speeds. Unfortunately, this analysis does not extend to frequencies above 1250 Hz due to limitations of the 1D model in accurately predicting higher frequencies.

4.5 Increase in orifice area

As previously mentioned, the VOPH exhibits lower inefficiencies compared to the VOCH. However, a significant advantage of utilizing VOPH is its potential to enhance the overall orifice passage area, by dedicating the entire cylinder head to the discharge orifice and using the piston head for the suction orifice. An analysis was conducted to assess a 100% increase in the orifice passage area with the VOPH, denoted as VOPH* in Fig. 13.

Fig. 13a, clearly shows that despite te substantial 100% increase in orifice area, the VOPH* configuration does not exceed the exergetic efficiency of the conventional VOCH. This indicates that the reductions of head loss are insufficient to compensate for the increased heat transfer losses. However, at higher rotational speeds, where head loss is more significant than heat transfer, the efficiencies of VOCH and VOPH* become similar. As depicted in Fig. 13b, the same trends are observed in volumetric efficiency. At intermediate rotational speeds, specifically at $N^* = 0.7$ and $N^* = 0.75$, the volumetric efficiencies of both VOPH and VOPH* approach each other, due to the increased suction orifice area reducing supercharging effects.

5. CONCLUSIONS

The aim of this study was to compare the performance of compressors with suction valves mounted on the cylinder head (VOCH) and on the piston (VOPH). The findings revealed negligible differences in valve displacements for both configurations at low speeds, corroborating previous research. However, at higher speeds, the VOPH showed greater displacement and opened slightly earlier that the VOCH. However, subsequent valve oscillations revealed that the VOPH had a smaller displacement compared to the VOCH. The study also examined the volumetric inefficiencies associated with the suction process. The piston configuration was found to introduce higher inefficiencies due to the inertial effects of the piston motion. Consequently, the volumetric efficiency of the VOPH configuration was found to be consistently lower than that of the VOCH, due to increased losses during the suction process. Overall, the tested valve configurations did not significantly affect exergy loss. However, the choice of valve configuration should consider heat transfer irreversibility, as it can significantly affect the exergetic efficiency. These findings provide valuable insights for optimizing compressor design with varying valve configurations.

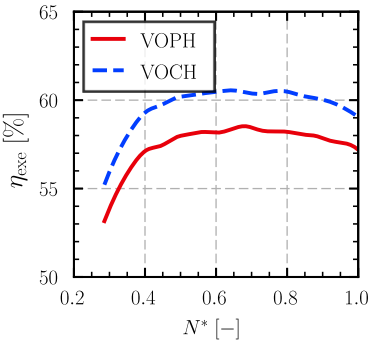

Figure 11 - Exergetic efficiency for both valve configurations.

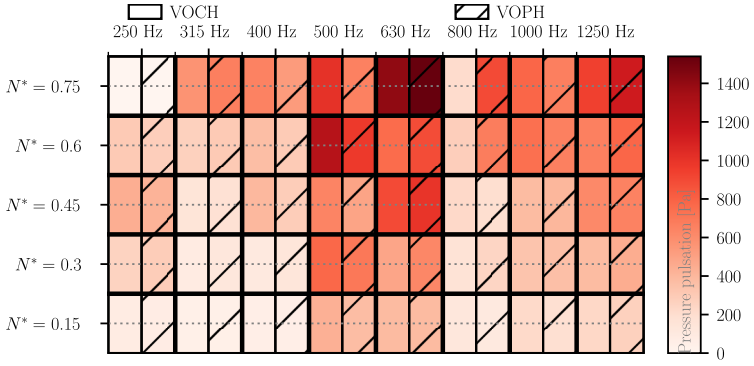

Figure 12: Acoustic performance for both valve configurations.

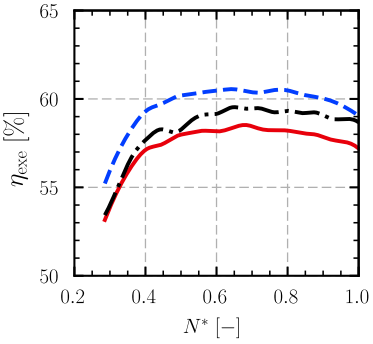

(a) Exergetic efficiency

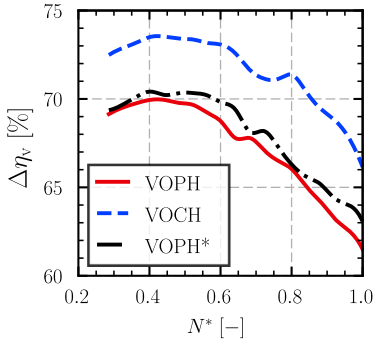

(b) Volumetric efficiency

Figure *13* - Overall exergetic efficiency (a) and volumetric efficiency (b) for the compressor with VOPH, VOCH, and with VOPH with 100% of increase in the orifice area

NOMENCLATURE

η	efficiency	(–)
I	specific exergy loss	(kJ/kg)
N	rotational speed	(rpm)
N^*	dimensionless rotational speed	(–)
RMSE	root mean square error	(–)
SV1	suction valve 1	

SV2	suction valve 2	
u^*	dimensionless impact velocity	(–)
VOCH	valve on the cylinder head	
VOPH	valve on the piston head	
x	piston displacement	(mm)
y	valve displacement	(mm)

Subscript

b	suction backflow
exe	exergetic
ht	heat transfer
rev	reversible
sch	supercharging
suc	suction process
sv	suction valve
v	volumetric

REFERENCES

Araujo, I. M.; Deschamps, C. Exergy Analysis of Hermetic Reciprocating Compressors Adopted in Household Refrigeration Systems. In: Proc. 18th Brazilian Congress of Thermal Sciences and Engineering. 2020.

Deschamps, C. J.; Possamai, F. C.; Pereira, E. L. L. Numerical Simulation of Pulsating Flow in Suction Mufflers. In: Proc. Int. Compressor Engineering Conference., 2002.

Disconzi, F. P.; Deschamps, C. J.; Pereira, E. L. Development of an In-Cylinder Heat Transfer Correlation for Reciprocating Compressors. In: Proc. Int. Compressor Engineering Conference at Purdue., 2012.

Lemmon, E. W.; Bell, I. H.; Huber, M. L.; Mclinden, M. O. Nist Standard Reference Database 23: Reference Fluid Thermodynamic and Transport Properties-Refprop, Version 10.0, National Institute of Standards And Technology. Standard Reference Data Program, Gaithersburg, 2018.

Link, R.; Deschamps, C. J. Numerical Analysis of Transient Effects on Effective Flow and Force Areas of Compressor Valves. In: Proc. Int. Compressor Engineering Conference., 2010.

Pereira, E. L.; Deschamps, C. J. Influence of Piston on Effective Areas of Reed-Type Valves of Small Reciprocating Compressors. HVAC and R Research, V. 17, P. 218–230, 4 2011.

Pizarro-Recabarren, R. A.; Barbosa, J. R.; Deschamps, C. J. Modeling the Stiction Effect in Automatic Compressor Valves. Int. J. Refrigeration, V. 36, P. 1916–1924, 11 2013.

Santos, L. M.; Deschamps, C. J. Characterization of Volumetric Inefficiencies of Reciprocating Compressors Adopted in Small Capacity Refrigeration Systems. In: Proc. 18th Brazilian Congress of Thermal Sciences and Engineering, 2020.

Silva, W. T. F. D. da; Yupa-Villanueva, R.; Deschamps, C. J. Numerical Analysis of Volumetric Inefficiencies of a Small Variable Capacity Reciprocating Compressor. In: Proc. 19th Brazilian Congress of Thermal Sciences and Engineering, 2022.

Wu, W.; Guo, T.; Peng, C.; Li, X.; Li, X.; Zhang, Z.; Xu, L.; He, Z. FSI Simulation of the Suction Valve on the Piston for Reciprocating Compressors. Int. J. Refrigeration, V. 137, P. 14–21, 2022.

ACKNOWLEDGEMENT

The authors acknowledge the support from Nidec-GA and EMBRAPII for the project “Analysis of the Performance of Reciprocating Compressor Components for Increased Reliability and Efficiency”. Additional funding was provided by the National Institutes of Science and Technology (INCT) Program, under CNPq Grant No. 404023/2019-3 and FAPESC Grant No. 2019TR0846.